

## Microstructure behavior and metal flow during continuously extending-extrusion forming of semisolid A2017 alloy

GUAN Ren-guo(管仁国), WEN Jing-lin(温景林), WANG Shun-cheng(王顺成), LIU Xiang-hua(刘相华)

School of Materials and Metallurgy, Northeastern University, Shenyang 110004, China

Received 25 May 2005; accepted 8 August 2005

**Abstract:** A self-designed test machine of continuously semisolid extending extrusion was made to produce the flat bar of A2017 alloy. The slurry of A2017 alloy with spherical or elliptical structures was obtained. During manufacturing semisolid A2017 alloy by the proposed process, the spherical grain was formed with the application of the large force provided by the rough roll. By controlling the casting temperature, the products of A2017 alloy with fine surfaces and rectangular transections of 14 mm×25 mm were produced. The microstructure of the product is fine with the stripped appearance. The fracture strength and elongation of the product are increased by 100 MPa and 29%, respectively.

**Key words:** A2017 alloy; semisolid alloy; slurry; extending extrusion; flat bar; microstructure

### 1 Introduction

Semisolid metal forming process is a kind of near-net-shape technology and attracts attentions all over the world[1–4]. Most available semisolid processes involve several technical steps: manufacturing semisolid slurry, remelting of semisolid slab and semisolid forming. Many scientists try to combine organically above technical steps as a convenient way of near-net-shape forming[5–15]. As shown in Fig.1, through the proposed process, manufacturing semisolid alloy and extending extrusion can be organically combined. The molten alloy was stirred by the rotating roll, and transformed into semisolid slurry, then, was drawn downward by the roll. An extending forming mould was installed at the exit of the roll-shoe gap. A2017 alloy was continuously extruded at the semisolid state[6–10]. The process has the following advantages: 1) Manufacturing semisolid slurry and continuously forming are organically combined; 2) The microstructure and properties of the products are excellent; 3) It is a new process to produce large sectional bar. At the present, the available processes of producing large transect materials require large extrusion machines, so the fabrication cost is very high. The proposed process can obviously reduce the cost. In

this paper, based on the self-made test machine, the continuously semisolid extending extrusion of producing flat bar of A2017 alloy was investigated.

### 2 Experimental

The experimental setting was a self-made test machine with the design parameters: the roll radius  $R_0=150$  mm, the shoe curvature  $R_1=154$  mm, the roll-rotating velocity  $v_0=0.2$  m/s, the roll-shoe gap width  $B=4$  mm and the angle size on the circle of the shoe  $\theta=90^\circ$ . The cross-section size of the forming region was 14 mm×25 mm. The test material was A2017 alloy, which has a wide semisolid temperature zone with the solidus and liquidus of 513 °C and 641 °C, respectively. The alloy was refined at 790 °C before carried to the test machine. The molten alloy was poured into the roll-shoe gap at a casting temperature of 690, 710, 730, 750, 770 and 790 °C, respectively, and was stirred by the rotating roll and transformed into semisolid slurry. Finally, the semisolid alloy was extruded by the mould installed at the exit of the roll-shoe gap, as shown in Fig.1. After the roll stopped during the pouring operation, subsequently, the alloy that remained in the roll-shoe gap and mould solidified, then, specimens were taken from different locations of the roll-shoe gap. The solidified alloy in the

filling mouth, extending cavity and forming zone were taken out as a whole. After the alloy was polished and etched, the features of microstructure evolution and metal flow of the alloy were investigated. The microstructure of solidified A2017 slurry was also observed. Finally, the microstructure and properties of the product were studied with optical microscope, X-ray diffractometer and material tensile machine.

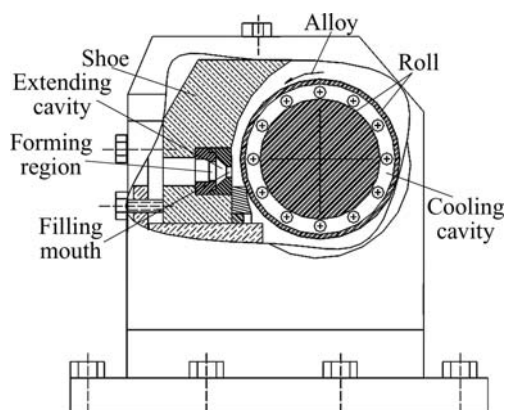


Fig.1 Schematic diagram of test machine

### 3 Results and discussion

#### 3.1 Microstructure formation of slurry

During manufacturing semisolid A2017 alloy by the proposed process, the spherical grain was formed with the application of large force provided by the rough roll. The spherical grain formation can be divided into two steps: free grain formation and free grain growth. At the initial stage of the solidification, A2017 alloy nucleates on the roll surface. The features of the roll surface obviously affect the nucleation rate of the molten alloy. According to the nucleation energy  $\Delta G = \Delta G_0(2 + \cos\theta)(1 - \cos\theta)^2/4$ , when the wetting angle  $\theta$  is small, the nucleation energy  $\Delta G$  is also small, so the dendrites can easily grow on the roll surface, which will cause a large quantity of free grains to form by the shearing. So the wetting ability of the roll surface is an important factor for the free grain formation. With the polished roll surface and at the casting temperature of 730 °C, because the roll surface was smooth and the wetting ability was poor, it was difficult for free grain formation[8]. However, when the roll surface was rough, lots of dendrites were obtained on the roll surface, which was described elsewhere[8]. Fig.2 shows the microstructure evolution in the roll-shoe gap at the casting temperature of 730 °C. The primary dendrite arms are crushed into small fractions by the shearing force of the roll, then, the small fractions disperse in the melt and grow as the free grains. According to the tests, the roll can provide a large shearing torque up to 18 950

N·m, while the heat convection is relatively small. So it is considered that the dendrite fragmentation is caused by the following mechanisms: 1) Dendrite arms are sheared off from main bodies at their roots, due to the large shearing force provided by the roll, lots of free grains from shearing-broken dendrites that look like rosettes are observed, as shown in Fig.2(b); 2) Remelting of the arms at their roots as a result of normal ripening, which can be proved by a fact that there are lots of deformation arms with the bending angles above 20° (location A in Fig.2(b)). The effect of fluid flow in this case is to alter or accelerate the solute diffusion involved in ripening and to carry the dendrite arm from its mother grain to where it can grow as a free grain.

While the free grains grow freely under the roll's shearing, their structure changes. Because that the heat diffusion normal to the roll surface is dominant, grains prefer to grow along this direction. However, inasmuch as the roll is rotating, the alloy is sheared and moves freely with slipping and rotating. So in this case, there are internal frictions, convection and solute congregation. As a result, the dendrite arms are sheared off from main bodies at their roots, as shown in Fig.2. On the other hand, free grains' rotating will cause the alternation of the heat diffusion direction. At the same time, solute diffusion, convection and the heat diffusion can cause the change of temperature and composition on the surface of the free grains, which causes the growth direction to alter continuously. So the free grains have equal chance to grow in every direction and grow into the equiaxed or spherical particles.

At position *a*, the internal structure maintained in the gap is shown in Fig.2(a). The equiaxed dendrites are very bigger. However, it can be observed in Fig.2(b) that lots of grains have already evolved to rosette structures at the location *b*. When the alloy is dragged downwards constantly it is sheared and cooled further. As a result, nearly all of the free grains evolve to spherical or elliptical structures, as shown in Fig.2(c). When the alloy comes out of the roll-shoe gap, its microstructure (Fig.2(d)) is mainly composed of spherical or elliptical structures.

The microstructures of the alloy at different casting temperatures are shown in Fig.3. When the casting temperature is in the range of 690–750 °C, the grain size distributes in the range of 10–40 μm.

#### 3.2 Metal flow of alloy during deformation process

The flow velocity of the alloy is maximal in the center of mould and decreases gradually from the center to the sides of the mould, as shown in Fig.4(a). This phenomenon can also be found by the simulation represented in Refs.[7, 9]. The alloy homogeneously fills

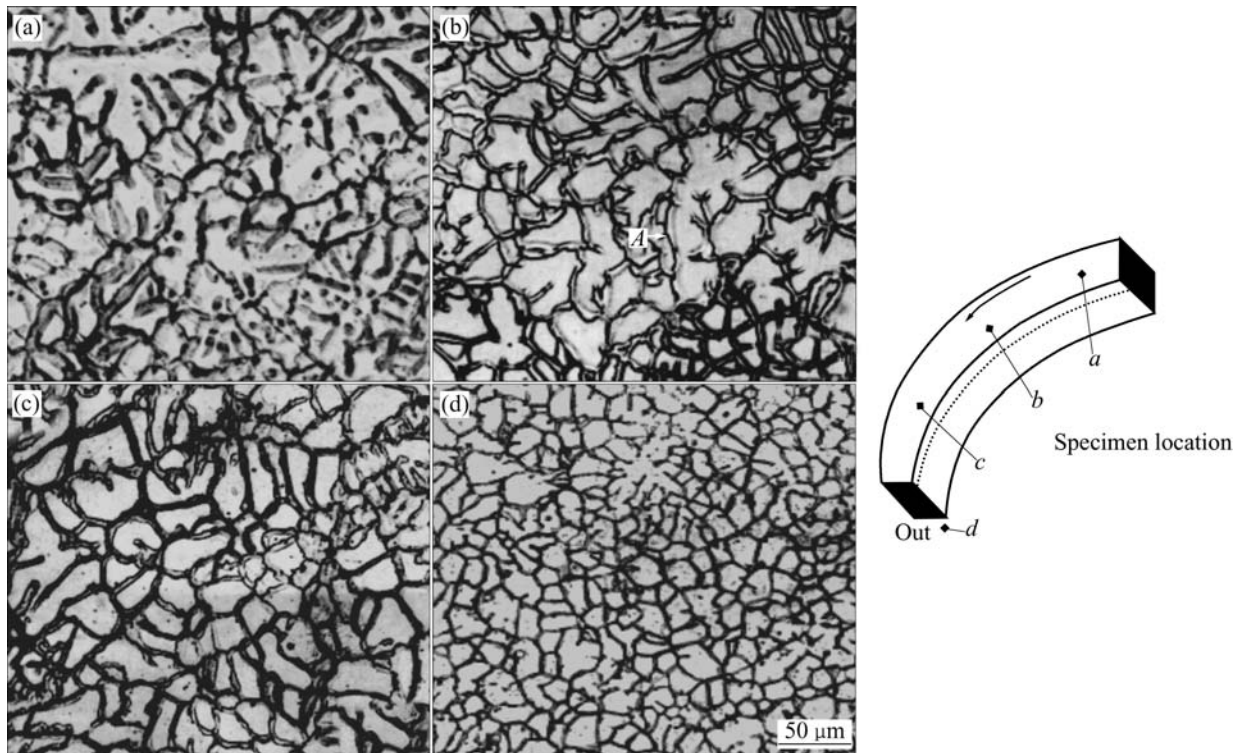


Fig.2 Microstructure evolution in and out of roll-shoe gap (right picture shows specimen location)

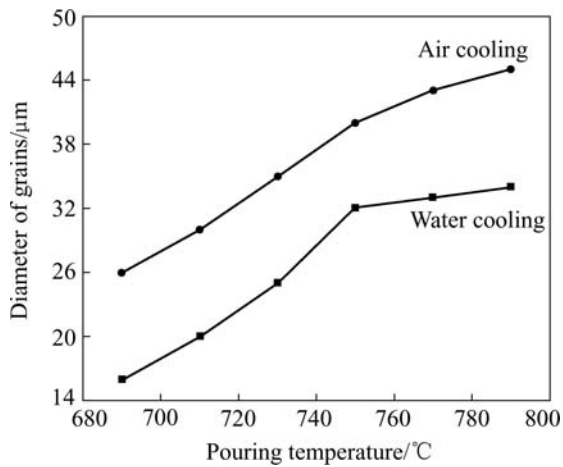


Fig.3 Relationship between casting temperature and grain size

the extending cavity with an elliptical pattern along the normal direction to the inside surface of the extending cavity, the flow lines of the alloy looks like the planetary orbits, which are shown in Fig.4(b). The resistance force including the friction force by the mould wall and the cling force between different alloy layers is very small in the center. As a result, the flow velocity of the alloy in the center is maximal. The two corners at the bottom of the mould are called the dead space where the alloy flow velocity is almost zero.

The casting temperature greatly affects the stability of the forming process. When the casting temperature exceeds 770 °C, the temperature of product at the exit of the mould is very high, thus the solid fraction is even

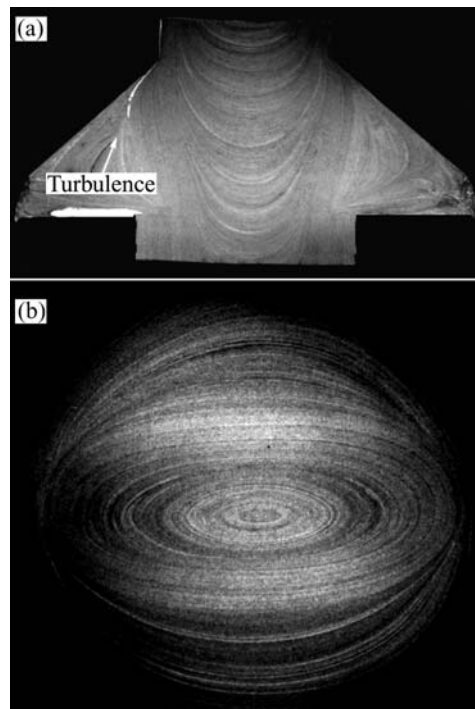


Fig.4 Metal flow lines in extending-extrusion mould: (a) Whole section; (b) Transverse section

lower than 0.90. The liquid is extruded out to the surface of the product, which will cause the product broken. In this case, the product surface is usually rough with many cracks, as shown in Fig.5(a).

High casting temperature can cause the alloy to fill the mould with a small solid fraction. After it is extruded

out from the mould, there is still much liquid in it. The liquid constantly extrudes out of the product surface and contacts with the sidewall of the forming mould, as schematically shown in Fig.6, and then the alloy easily clings to the forming mould. This kind of clinging results in a tension stress  $\sigma_v$  in the product surface. The tension stress strongly depends on the shearing force in the alloy, and can be illustrated by the equation:

$$\tau_{ij} = -\mu \left[ \frac{\partial U_i}{\partial x_j} + \frac{\partial U_j}{\partial x_i} \right]$$

where  $\tau_{ij}$  is the shearing stress in the alloy,  $\mu$  and  $U$  are the viscosity and the displacement of the alloy, respectively. It is seen that the shearing force in the alloy

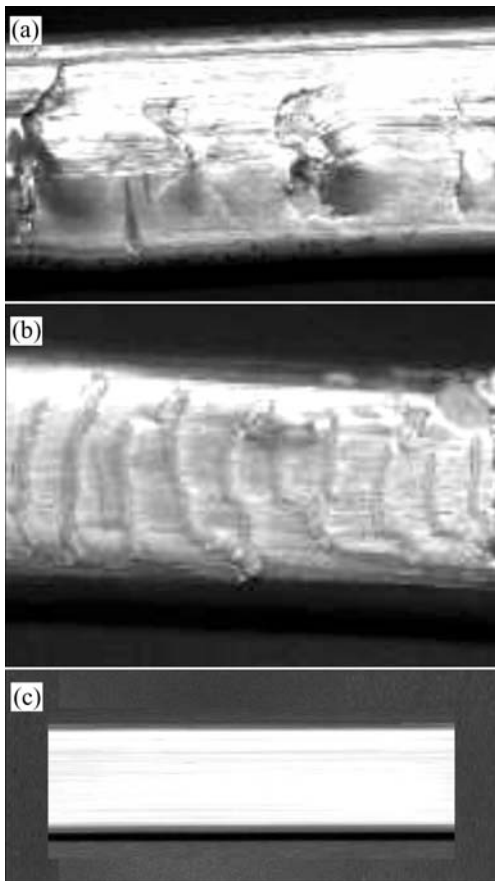


**Fig.5** Surfaces of product: (a) Cracks; (b) Cracks and periodical wavelike surface; (c) Smooth surface

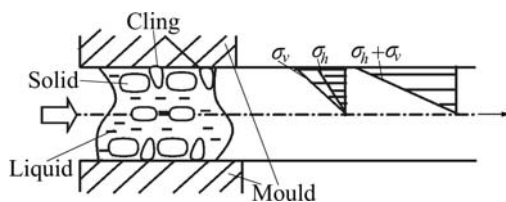


**Fig.6** Clinging of alloy on mould surface and stresses in surface of product

is related to the alloy viscosity. The results by computer simulation show that when the casting temperature is in the range of 690-790 °C, the solid fraction of the alloy in the forming region is more than 85% [7, 8], which means that the high temperature not beyond 790 °C will cause great viscosity at the forming region, and will cause great tension stress  $\sigma_v$ . Moreover, high casting temperature can cause a great thermal stress in the alloy surface. Inasmuch as the central temperature is higher than the surface temperature, the thermal stress in the alloy surface  $\sigma_h$  appears with a pattern of tension stress, as shown in Fig.6. The overlapped stress of two kinds of tension stresses  $\sigma_v + \sigma_h$  is very large on the surface of the alloy, which is shown in Fig.6. The overlapped stress can cause the rough surface of the product.

On the contrary, when the casting temperature is lower than 690 °C, the alloy inhomogeneously fills the extending mould with a high solid fraction, and then the sharp turbulence occurs, there are some flaws in the product such as segregation, cracks and periodically wavelike surfaces, as shown in Fig.5(b). At low casting temperature, in the case of casting at 690 °C, the solid fraction in the forming region is very high and even reaches 100%. So the yield strength of the alloy is very large. In this case, if the torque provided by the electric motor cannot meet the requirements for the metal flow, the test machine will not work. Also, because the alloy contacts with the mould, the temperature in the center of the alloy is higher than that at the surface. Therefore, the alloy flows relatively easily in the center. In addition, the friction force and the clinging force are imposed on the outsides of the alloy by the mould wall. Both reasons cause the alloy to flow non-uniformly. Meanwhile, because of the resistance force by the mould, the alloy accumulates on the surface. So the maximal resistance appears at the forming region. This force becomes larger and larger with the accumulation of the alloy. But once it reaches a tolerant limit, the accumulated alloy will be torn and flow out of the mould all-together, and a new accumulation of the alloy will occur. Then, this kind of accumulation-flow cycle will go on, which will cause the periodical waves on the surface of the product as shown in Fig.5(b).

The solid fraction depends on the temperature of the alloy, so one convenient way is to control the casting temperature. Under the present experimental conditions, it is shown that when the casting temperature is between 710 °C and 750 °C, the alloy flows soundly, and the product of A2017 alloy with smooth surface and rectangular transection of 14 mm×25 mm is obtained, as shown in Fig.5(c).

**3.3 Microstructure and properties of product**

Fig.7 shows the microstructures of the product

when cast at 710 and 730 °C. It can be seen that the microstructure of the product is fine and homogeneous with a striped appearance. The black zone is composed of phases with lower melting points. Through X-ray analysis, it is shown that the main component is  $\text{CuAl}_2$ . The black striped structure is formed during the solidification of the liquid phase. The white phases are  $\alpha$  base phases that are stretched during the forming process. When the casting temperature is lower than 710 °C, many  $\alpha$  solid phases precipitate during the forming process and aggregate easily, therefore, the microstructure is large. While the casting temperature is relatively high, the aggregated mass is small. Under the present conditions, the casting temperature between 710 °C and 750 °C is suggested.

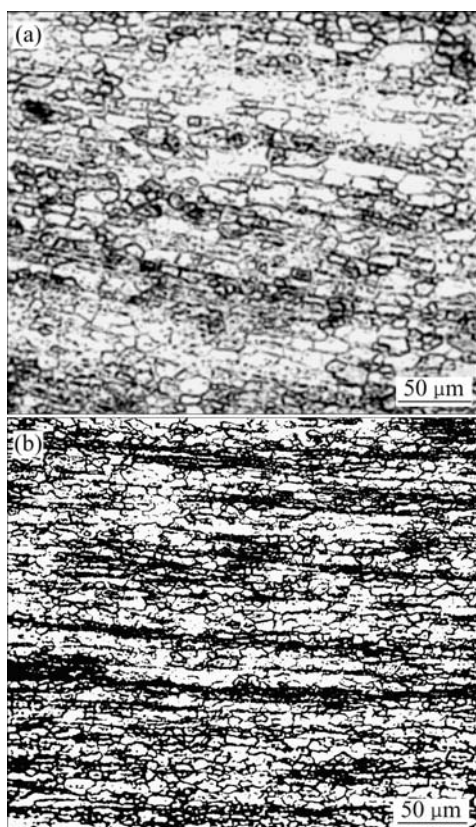


**Fig.7** Microstructures of product of A2017 alloy at different casting temperatures: (a) 710 °C; (b) 730 °C

Five specimens taken from the products at the casting temperature of 730 °C were elongated at room temperature, and the deformation speed was  $0.1 \text{ s}^{-1}$ . Comparing to the national standard, the fracture strength and elongation of the product of A2017 alloy are improved by 100 MPa and 29%, respectively.

## 4 Conclusions

1) A self-designed test machine of continuously semisolid extending-extrusion was made to produce the flat bar of A2017 alloy. During manufacturing the semisolid A2017 alloy by the proposed process, the spherical grain formation was observed with the application of large force provided by the rough roll.

2) Under the present experimental conditions, the casting temperature range of 710-750 °C was suggested to produce A2017 product with the good surface quality.

3) The microstructure of the product is fine with the striped appearance. The fracture strength and elongation of the product are improved by 100 MPa and 29%, respectively.

## References

- [1] FLEMINGS M C. Behavior of metal alloys in the semisolid state[J]. *Metal Trans*, 1991, 22A(1): 957-981.
- [2] KIRKWOOD D H. Semisolid metal processing[J]. *International Materials Reviews*, 1994, 39(5): 173-189.
- [3] HAGA T. Semisolid strip casting using a twin roll caster equipped with a cooling slope[J]. *J Mater Proc Tech*, 2002, 130(2): 558-561.
- [4] HAGA T, KENTA T, MASAOKI I. Twin roll casting aluminum alloy strips[J]. *J Mater Proc Tech*, 2004, 153(2): 42-47.
- [5] HAGA T, KAPANOS P. Thixoforming of laminate made from semisolid cast strips[J]. *J Mater Proc Tech*, 2004, 157(2): 508-512.
- [6] KIUCHI M, SUGIYAMA S. A new process to manufacture semi-solid alloys[J]. *ISIJ International*, 1995, 35(6): 790-796.
- [7] GUAN Ren-guo, WEN Jing-lin, LIU Xiang-hua. FEM analysis of aluminum AA2017 alloy thermal/fluid multiple fields during a single-roll stirring process[J]. *Mater Sci and Tech*, 2003, 19(4): 503-508.
- [8] GUAN Ren-guo, WEN Jing-lin, LIU Xiang-hua, MENG Xian-yun. Continuously extending extrusion forming of semisolid A2017 alloy by SCR process[J]. *Rare Metals*, 2002, 21(4): 271-275.
- [9] GUAN Ren-guo, LI Ying-long, WANG Shun-cheng, WEN Jing-lin. Finite element modeling analysis of metal flowing during process of extending extruding semisolid A2017 alloy[J]. *The Chinese Journal of Nonferrous Metals*, 2004, 14(9): 1539-1544. (in Chinese)
- [10] ZHANG Bin, LI Mo-lin, WANG Feng-gang. Calculation of extending extrusion force on extending cavity sides[J]. *Metal Forming Technology*, 1996, 14(4): 31-35.
- [11] MAO Wei-min, ZHAO Ai-min, YUN Dong, ZHONG Xue-you. Preparation study of semisolid 60Si2Mn spring steel slurry[J]. *Acta Metallurgica Sinica*, 2003, 16(6): 483-488.
- [12] MAO W M, ZHAO A M, ZHONG X Y. Spherical microstructure formation of the semisolid high chromium cast iron Cr20Mo2[J]. *Acta Metallurgica Sinica*, 2004, 17(1): 77-82.
- [13] GUAN Ren-guo, WEN Jing-lin, LIU Xiang-hua. Microstructure of remelted A2017 semisolid alloy with little hot deformation and its semisolid rolling[J]. *The Chinese Journal of Nonferrous Metals*, 2002, 12(5): 1002-1006. (in Chinese)
- [14] CHEN Z H, ZHANG H, KANG Z T. Thixoforming of 6066 aluminum alloy by multi-layer spray deposition[J]. *Trans Nonferrous Met Soc China*, 2001, 11(1): 108-114.
- [15] LIU D, CUI J, XIA Ke-nong. Non-dendritic structural 7075 aluminum alloy by liquidus cast and its semisolid compression behavior[J]. *Trans Nonferrous Met Soc China*, 2000, 10(2): 192-195.

(Edited by YUAN Sai-qian)